MT-Pallantia Publisher

Journal of Science with Technological Applications
ISSN: 0719-8647

Hydroxyapatite nanoparticles: an alternative as nanocarriers for sterol-derived drugs

Tulio A. Lerma [1,2], Manuel Palencia [3], Jhoban Meneses [1], Sixta L. Palencia-Luna [1,4], Keybi E. Mora [1]

[1] *Mindtech Research Group (Mindtech-RG), Mindtech s.a.s., Cali – Colombia.*
[2] *Technological Development Unit in New Materials (UDT-NM), Polymeiker S.A.S, Montería, Colombia.*
[3] *Research Group in Science with Technological Applications (GI-CAT), Department of Chemistry, Universidad del Valle, Cali – Colombia.*
[4] *Department of Nutrition and Dietetics, San Sebastian University, Concepción - Chile.*

Corresponding Author: Manuel Palencia. E-mail: manuel.palencia@correounivalle.edu.co

Graphical Abstract

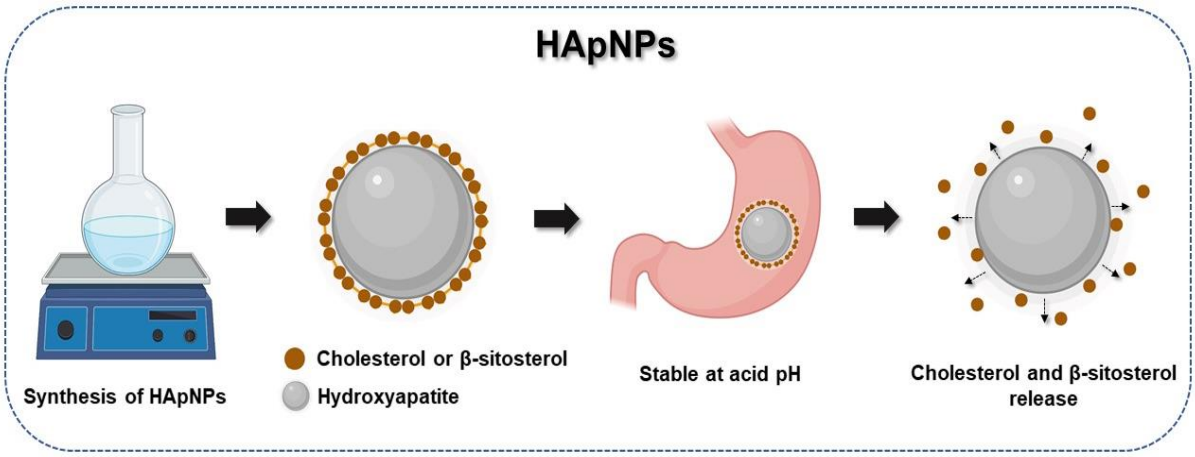

Abstract. Hydroxyapatite nanoparticles (HApNPs) are inorganic materials with sizes less than 100 nanometers. Their main characteristic is biocompatibility because their chemical composition is similar to human bone, making them suitable for use in physiological environments. These characteristics make them a promising alternative for the delivery of sterol-derived drugs, offering better targeting and controlled release compared to conventional drug delivery methods. In this study, HApNPs loaded with cholesterol and β-sitosterol were synthesized using the chemical precipitation method. The nanoparticles (NPs) were characterized by Fourier Transform Infrared (FTIR) spectroscopy to identify functional groups and confirm the presence of sterols on the HApNPs. The morphology and size of the NPs were analyzed using transmission electron microscopy (TEM) and dynamic light scattering (DLS). The loading amount of sterol derivatives was determined by thermogravimetric analysis, and the stability of the nanoparticles in an acidic medium was also evaluated. The results showed that HApNPs loaded with cholesterol and β-sitosterol were successfully synthesized, exhibiting a spherical morphology with diameters less than 100 nm. The data confirmed the incorporation of cholesterol and β-sitosterol on the surface of the HApNPs, and their subsequent release was also observed. Moreover, the presence of sterol derivatives in the nanobiointerface enhanced the nanoparticles' resistance to acidic conditions, suggesting their potential as drug nanocarriers for targeted release in the intestines without undergoing alterations during transit through the stomach.

Keywords: Hydroxyhapatite nanoparticles, cholesterol, β-sitosterol, interface, acid medium.

Cite as: Lerma T.A., Palencia M., Meneses J., Palencia-Luna S.L., Mora K. E. Hydroxyapatite nanoparticles: an alternative as nanocarriers for sterol-derived drugs. J. Sci. Technol. Appl., 21, 2024 (in JSTA 2026), Art-121, 1-7.
https://doi.org/10.34294/j.jsta.26.21.121

Accepted: 2024-06-25 | Published: 2024-08-10 | Paper Number: 121 (STEM) | Research Article

1. Introduction

Commercial drugs consist of an active ingredient, the molecule responsible for the pharmacological effect, and an excipient, which are inert substances used to facilitate the dosage and administration of the drug. However, these excipients can significantly impact the drug's efficacy. Many commercial drugs suffer from limitations in their pharmacological action, such as a lack of prolonged therapeutic effect and insufficient targeting of the site of action. These shortcomings can lead to increased medication consumption, raising the risk of high drug concentrations in the body. This can potentially disrupt the normal functioning of organs and lead to serious health consequences (Zhang et al., 2016). Currently, NPs have been developed to enhance the therapeutic efficacy of conventional drugs. NPs improve drug delivery, minimize side effects, and maximize treatment efficacy (Elumalai et al., 2024). The effectiveness of NPs in clinical treatments depends heavily on their characteristics, such as surface charge, chemical composition, size, and morphology, among others (Kwon, et al., 2018). Various types of NPs, including metallic, polymeric, and inorganic, have been explored for drug delivery applications. However, their chemical composition significantly impacts biological interactions. For example, copper nanoparticles (Cu NPs) have been studied to deliver doxorubicin in cancer treatment, showing a potent cytotoxic effect (Li et al., 2017). However, recent studies have indicated that metallic NPs, can cause genotoxic effects, limiting their suitability for clinical applications (Barabadi et al., 2019).

Inorganic NPs composed of safe components, such as hydroxyapatite (HAp), are notable for their biocompatibility. HAp is the main inorganic component of teeth and bones in vertebrate animals (Yu et al., 2014). From a biomedical perspective, HApNPs are highly valued for their structural similarity to human bone, ability to stimulate bone regeneration, and stability in physiological environments. The synthesis of HApNPs has enabled the creation of biocompatible compounds for use in constructing biological markers or drugs. Depending on the synthesis method used, these nanomaterials can exhibit various morphologies, allowing for precise control of the interface between the NPs and their surroundings (Swain et al., 2012). Several methods are available for synthesizing HApNPs. The chemical precipitation method produces spherical NPs by reacting diammonium phosphate with calcium nitrate in an alkaline medium. Alternatively, the hydrothermal method can yield rod-shaped NPs using the same precursors but involves processing in a hydrothermal reactor at 200 °C for 24 to 72 hours (Dědourková et al., 2012; Gopi et al., 2012).

The biocompatibility of HAp with the human body presents a promising alternative for the design of drug-loaded NPs to serve as vehicles for targeted drug delivery and controlled release. HApNPs have been utilized for drug release, exemplified by their use in loading antibiotics for deposition on dental implants (Geuli et al., 2017). Another example is the use of hollow HApNPs to deliver doxorubicin (DOX), a therapeutic anticancer drug. These NPs have demonstrated high drug-loading efficiency (93.7 %) and significantly reduced the viability of BT-20 cancer cells by approximately 20 % in MTT (3-(4,5-dimethylthiazol-2-yl)-2,5-diphenyltetrazolium bromide) assays (Yang et al., 2013). Additionally, HApNPs are highly sensitive to pH changes, with the NPs dissolving and releasing the drug more effectively in acidic environments (~80 %). This is a particularly important characteristic for cancer treatment, as cancer cells typically exhibit lower pH levels than normal cells (Pan et al., 2018). This pH sensitivity allows for enhanced drug release in the acidic microenvironment of cancer cells, making HApNPs a valuable tool for targeted cancer therapy. However, despite their promising properties, HApNPs exhibit high instability in aqueous solutions, resulting in an unstable colloid system (Moreno et al., 1968). HApNPs can be stabilized by adsorbing hydrophobic molecules onto their surface to address this issue. For instance, skim milk has been used to disperse HApNPs effectively, demonstrating its ability to maintain dispersion and protect the NPs, thereby reducing their dissolution in acidic conditions (Choki et al., 2021).

On the other hand, cholesterol and β-sitosterol have also been tested to modify the interface of NPs. This strategy not only increases the affinity of the nanomaterial for lipidic membranes but also acts as a protective layer against the acidic environment of the stomach (de S. L. Oliveira et al., 2020). Given these benefits, cholesterol and β-sitosterol are promising candidates for stabilizing the interface of HApNPs. In studies involving mice, β-sitosterol intake has shown improvements in fatty liver disease and a reduction in cholesterol levels, and it has been associated with the prevention of cardiovascular diseases. Furthermore, these molecules serve as the basis for various drugs (Feng et al., 2018). Therefore, based on the advantages of cholesterol and β-sitosterol in modifying the surface of nanomaterials, this research proposes a new methodology for synthesizing HApNPs stabilized with cholesterol (HApNPs-Cholesterol) and β-sitosterol (HApNPs-β-Sitosterol) via the precipitation method. These stabilized NPs are intended to be applied as potential drug nanocarriers. The HApNPs were analyzed using FTIR to assess functional groups. Additionally, the size and morphology of the NPs were determined using TEM and DLS.

2. Methodology

2.1. Materials

Calcium nitrate ($Ca(NO_3)_2$, 99 %), disodium phosphate (Na_2HPO_4, 99 %), and ammonia solution (NH_4OH, 25 %) were purchased from Merck. Hydroxyapatite (HAP), cholesterol ($C_{27}H_{46}O$, 92.5 %), β-sitosterol ($C_{29}H_{50}O$, 70 %), isopropanol (C_3H_8O, 99.5 %), and chloroform ($CHCl_3$, 99.5 %) were obtained from Sigma-Aldrich. Distilled water was used to prepare the aqueous solutions of calcium nitrate and disodium phosphate.

2.2. Synthesis of HApNPs

The HApNPs were synthesized using the chemical precipitation method in a mixture of water and chloroform. The procedure began

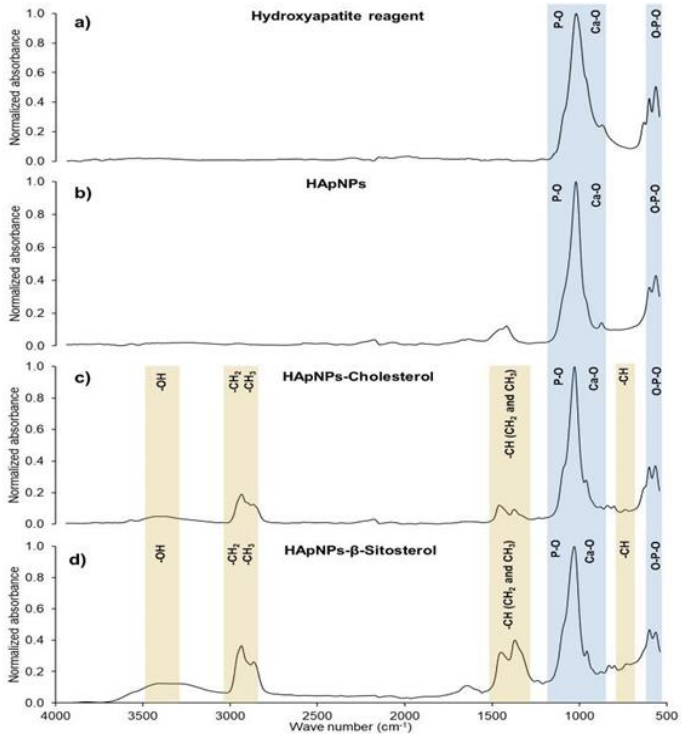

Figure 1. FTIR spectra of: a) reagent grade hydroxyapatite, b) HApNPs without stabilizing agent, c) HApNPs stabilized with cholesterol and d) HApNPs stabilized with β-sitosterol.

by preparing the first solution: 354.2 ± 0.1 mg of $Ca(NO_3)_2$ was dissolved in 10.0 mL of distilled water, and 1.0 mL of ammonia at a concentration of 25 % (v/v) was added. This solution was then transferred to a test tube and vigorously mixed with the respective sterol derivative solution at room temperature. Specifically, 376.0 ± 0.1 mg of cholesterol was dissolved in 10.0 mL of chloroform, and 533.1 ± 0.1 mg of β-sitosterol was dissolved in 10.0 mL of chloroform. Next, another solution was prepared by dissolving 127.8 ± 0.1 mg of Na_2HPO_4 in 10.0 mL of distilled water, followed by the addition of 1.0 mL of ammonia (25 %). This second solution was added dropwise to the first solution to form HApNPs-Cholesterol and HApNPs-β-Sitosterol. The mixture was then heated at 90 °C while stirring for 1 hour and 30 minutes. After cooling, the solution was centrifuged at 5000 rpm for 10 minutes using a Universal 320R-Hettich centrifuge. This washing procedure was repeated three times with 30.0 mL of distilled water each time. Finally, the precipitate was collected and dried at 90 °C for 3 hours, after which it was ready for further characterization and testing.

2.3. HApNPs characterization

The characterization of the HApNPs was performed using several techniques:

Fourier Transform Infrared Spectroscopy (FTIR): This was used to identify the functional groups of the stabilizing agents and HAp, with measurements taken in the range of 4000 cm^{-1} to 500 cm^{-1} using an ATR-IR Affinity-1S spectrophotometer (Shimadzu). FTIR was also employed to verify the presence and release of sterols.

Dynamic Light Scattering (DLS): The hydrodynamic diameter of the NPs was measured using a Zetasizer Lab (Malvern) at 25 °C in isopropanol.

Transmission Electron Microscopy (TEM): The size and morphology of the NPs were analyzed using a JEM-1011 microscope (JEOL) with an accelerating voltage of 80 kV.

2.4. Determination of Cholesterol and β-Sitosterol Content in the HApNPs and Release Assay

The content of cholesterol and β-sitosterol in the NPs was determined using Thermogravimetric Analysis (TGA) on a TA Instruments Q-50. The analysis was conducted over a temperature range of 30 °C to 900 °C with a heating ramp of 10 °C/min under a nitrogen atmosphere.

For the sterol release assay, the NPs were subjected to chloroform at room temperature, with agitation at 1200 rpm for 30 minutes. After this, the particles were allowed to settle, filtered, and dried at 90 °C. The amount of sterol lost was calculated by measuring the mass difference. Additionally, to simulate gastric conditions, the nanoparticles were exposed to 0.1 N HCl at 37 °C to assess the concentration of calcium released from the hydroxyapatite (Gray et al., 2014).

3. Results and discussion

To evaluate the success of the HApNPs surface modification, FTIR spectra were obtained for HApNPs, HApNPs-Cholesterol, and HApNPs-β-Sitosterol (see **Figure 1**) and compared to the HAp reagent. In the spectra of HAp and HApNPs (see **Figure 1a** and **1b**), an intense band associated with the stretching vibrations of the P-O and Ca-O bonds was observed at 1026 cm^{-1} and 1020 cm^{-1}, respectively. Additionally, signals at 563 cm^{-1} and 599 cm^{-1} for HAp and 561 cm^{-1} and 599 cm^{-1} for HApNPs correspond to the bending vibrations of the O-P-O bond (Castro et al., 2022). These bands, related to P-O and Ca-O bonds, also appeared in HApNPs-Cholesterol (see **Figure 1c**) at 1027 cm^{-1} and HApNPs-β-Sitosterol (see **Figure 1d**) at 1031 cm^{-1}. The O-P-O vibration band was observed at 565 cm^{-1} and 599 cm^{-1} for HApNPs-Cholesterol, and at 565 cm^{-1} and 601 cm^{-1} for HApNPs-β-Sitosterol, indicating that cholesterol and β-sitosterol did not affect the HApNPs composition. These findings are consistent with those reported by (Venkatesan et al., 2015) for HApNPs derived from salmon fish bone.

In the stabilized HApNPs, signals associated with the functional groups of cholesterol and β-sitosterol were observed: around 3400 cm^{-1} for -O-H vibrations, in the range of 2950 cm^{-1} to 2800 cm^{-1} for symmetric and asymmetric stretching of CH_2 and CH_3 groups, and in the range of 1460 cm^{-1} to 1350 cm^{-1} for deformation vibrations of C-H bonds in methyl and methylene groups. Additionally, vibrations around 800 cm^{-1} were attributed to the deformation of C-H bonds. These results confirm the presence of cholesterol and β-

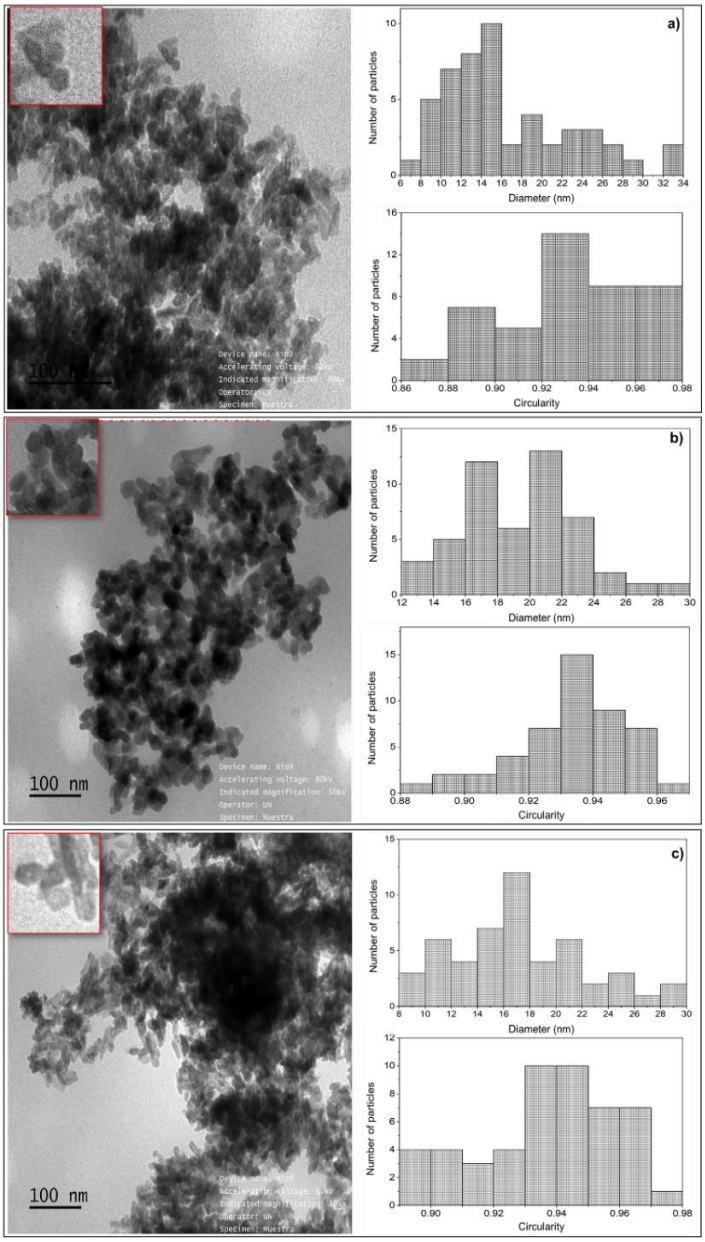

Figure 2. TEM images, diameters and circularity of: a) HApNPs without stabilizing agent, b) HApNPs stabilized with cholesterol and c) HApNPs stabilized with β-sitosterol.

sitosterol in the synthesized nanoparticles. The size of the HApNPs, HApNPs-Cholesterol, and HApNPs-β-Sitosterol was analyzed using TEM. **Figure 2** shows the TEM images, diameter distribution, and circularity distribution for the nanoparticles. The diameters of the HApNPs particles without a stabilizing agent ranged from 6 nm to 34 nm, with an average diameter of 16.5 ± 1.8 nm and a circularity of 0.91 (see **Figure 2a**).

For the HApNPs-Cholesterol, particle sizes ranged from 12 nm to 30 nm, with a mean diameter of 19.5 ± 1.0 nm and a mean circularity of 0.92 (see **Figure 2b**). The HApNPs-β-Sitosterol exhibited diameters between 8 nm and 30 nm, with a mean diameter of 17.3 ± 1.4 nm and a mean circularity of 0.93 (see **Figure 2c**). Thus, the classified as nanomaterials. The average circularity was above 0.90, obtained particles had diameters of less than 50 nm and can be indicating that the NPs are roughly spherical (Muscas et al., 2015). The TEM results were compared with those obtained from DLS. The hydrodynamic diameters measured by DLS were 257.2 ± 61.2 nm for HApNPs without a stabilizing agent, 152.5 ± 9.0 nm for HApNPs-Cholesterol, and 251.8 ± 12.1 nm for HApNPs-β-Sitosterol. The differences compared to TEM measurements are likely due to the agglomeration of the nanoparticles, as evidenced in the microscopy images. Additionally, DLS measures the hydrodynamic diameter, which includes agglomeration effects, leading to larger apparent sizes (Mulenos et al., 2020).

TGA determined the thermal stability of the HApNPs. According to the TGA results (see **Table 1**), the weight losses for HApNPs-Cholesterol were as follows: 1.97 % (30-144 °C), 37.96 % (144-340 °C), 13.57 % (340-610 °C), and 1.99 % (610-855 °C). These losses are attributed to sample moisture, cholesterol, impurities, and carbonate decomposition. Similar losses were observed for HApNPs-β-Sitosterol with degradation values of 2.19 % (30-144 °C), 55.67 % (144-355 °C), 10.50 % (355-610 °C), and 5.14 % (610-855 °C). To determine the content of sterol derivatives, the released or discharged sterols from the synthesized NPs were analyzed by TGA (see **Table 1**). This analysis helps correct the weight loss attributed to the HAp core, as demonstrated in the thermal analysis of HApNPs without a stabilizing agent. For HApNPs-Cholesterol, the first observed loss of 5.94 % (30-144 °C) corresponds to the sample's moisture content. The second loss of 2.61 % (144-340 °C) and the third loss of 1.90 % (340-610 °C) are associated with impurities, while the fourth loss of 1.90 % (610-855 °C) corresponds to carbonate decomposition. For HApNPs-β-Sitosterol, the losses were 3.24 % (30-144 °C), 2.88 % (144-355 °C), 2.84 % (355-610 °C), and 2.41 % (610-855 °C).

From the results obtained, it can be concluded that there is no significant presence of sterol derivatives in the NPs after the release or discharge assays, as no considerable weight loss was observed in the temperature range associated with sterol derivatives. Additionally, the percentages differ significantly when comparing the third loss between the thermograms of charged and uncharged NPs. This suggests that the third loss observed in the TGA of the charged NPs is not solely due to impurities such as nitrates and ammonium but also indicates the presence of sterols. These sterols are likely more integrated within the HAp cores, as reported with other materials (Maheen et al., 2022).

On the other hand, FTIR spectroscopy results of the released NPs showed only P-O, Ca-O, and O-P-O vibrations, along with signals between 1500 cm^{-1} and 1300 cm^{-1} corresponding to carbonate impurities, all associated with HAp (Castro et al., 2022). These findings indicate that no sterols are present and that they were su-

Table 1. TGA results for sterol reactants and HApNPs loaded and released from sterol derivatives.

Sample	Lost number	Temperature (°C)	Weight loss (%)	Observation
Cholesterol	1	144-339	100.00	Thermal degradation of cholesterol
β-Sitosterol	1	30-144	2.15	Water in sample
	2	144-354	97.85	Thermal degradation of β-Sitosterol
HApNPs without stabilizing agent	1	30-300	10.18	Water in sample
	2	300-655	6.31	Nitrate and ammonium waste
	3	655-855	0.95	Decomposition of carbonate in CO_2
HApNPs-Cholesterol	1	30-144	1.97	Water in sample
	2	144-340	37.96	Thermal degradation of cholesterol
	3	340-610	13.57	Nitrate and ammonium waste
	4	610-855	1.99	Decomposition of carbonate in CO_2
HApNPs-Cholesterol released	1	30-144	5.94	Water in sample
	2	144-340	2.61	Nitrate and ammonium waste
	3	340-610	1.90	Nitrate and ammonium waste
	4	610-855	1.90	Decomposition of carbonate in CO_2
HApNPs-β-Sitosterol	1	30-144	2.19	Water in sample
	2	144-355	55.67	Thermal degradation of β-sitosterol
	3	355-610	10.50	Nitrate and ammonium waste
	4	610-855	5.14	Decomposition of carbonate in CO_2
HApNPs-β-Sitosterol released	1	30-144	3.24	Water in sample
	2	144-355	2.88	Nitrate and ammonium waste
	3	355-610	2.84	Nitrate and ammonium waste
	4	610-855	2.41	Decomposition of carbonate in CO_2

ccessfully released from the NPs. This behavior is likely due to the solubilization of cholesterol and β-sitosterol in chloroform, which favors interactions between the molecules and the solvent over adsorption to the HApNPs (Šoltys et al., 2019). Regarding dissociation in an acidic medium, the HApNPs without a stabilizing agent showed 88.9 % dissociation in 5 minutes and 100.0 % in 15 minutes. In comparison, the HAP reagent dissociated 82.3 % in 5 minutes and 100.0 % in 25 minutes. These results suggest that the NPs degrade more quickly, likely due to their smaller size, which provides a larger surface area for interaction with the acid environment, making them more susceptible to degradation. In contrast, at 30 minutes, the HAP reagent and HApNPs without a stabilizing agent dissociated completely, while the HApNPs stabilized with cholesterol and β-sitosterol dissociated 29.7 % and 25.3 %. These results demonstrate that stabilizing agents, such as sterol derivatives, significantly reduce the dissociation of HApNPs in an acidic medium.

4. Conclusions

The HApNPs, HApNPs-Cholesterol, and HApNPs-β-Sitosterol, were successfully synthesized using a chemical precipitation method. FTIR analysis confirmed the presence of molecules of cholesterol and β-sitosterol on the nanoparticle's surfaces, with surface modification not affecting the HApNPs composition. TEM characterization revealed that the particles had diameters of less than 100 nm and exhibited a spherical morphology. The results showed that the inclusion of sterol derivatives, cholesterol and β-Sitosterol, did not alter the particle morphology. The thermogravimetric analysis demonstrated that the synthesized HApNPs could be loaded with sterol derivatives and subsequently released. The incorporation of these biomolecules enhanced the resistance of the inorganic cores to acidic environments. Thus, HApNPs with sterol derivatives hold promise as nanocarriers for oral delivery of sterol-derived drugs.

Conflict interest. The authors declare that there is no conflict of interest.

Acknowledgements. The authors acknowledge Mindtech s.a.s., Universidad del Valle, Polymeiker s.a.s., the Ministry of Science, Technology, and Innovation for project 80740-467-2021, and the Colombian National Planning Department, specifically the General Royalties System (SGR) for project BPIN2020000100261.

References

1. Barabadi, H., Najafi, M., et al. 2019. A systematic review of the genotoxicity and antigenotoxicity of biologically synthesized metallic nanomaterials: are green nanoparticles safe enough for clinical marketing? *Medicina*, *55*(8), 1-16. https://doi.org/10.3390/medicina55080439

2. Castro, M.A., Portela, T.O., et al. 2022. Synthesis of hydroxyapatite by hydrothermal and microwave irradiation methods from biogenic calcium source varying pH and synthesis time. *Boletín la Soc. Española Cerámica y Vidr*. 61, 35–41. https://doi.org/10.1016/j.bsecv.2020.06.003

3. Choki, K., Li, S., et al. 2021. Fate of hydroxyapatite nanoparticles during dynamic in vitro gastrointestinal digestion: the impact of milk as a matrix. *Food Funct*. 12, 2760–2771. https://doi.org/10.1039/D0FO02702B

4. Dědourková T., Zelenka, J. et al. 2012. Synthesis of sphere-like nanoparticles of hydroxyapatite. *Procedia. Eng*. 42, 1816–1821. https://doi.org/10.1016/j.proeng.2012.07.576

5. de S. L. Oliveira, A.L., dos Santos-Silva, A.M., et al. 2020. Cholesterol-functionalized carvedilol-loaded PLGA nanoparticles: anti-inflammatory, antioxidant, and antitumor effects. *J. Nanoparticle. Res*. 22, 2-14. https://doi.org/10.1007/s11051-020-04832-8

6. Elumalai, K., Srinivasan, S., et al. 2024. Review of the efficacy of nanoparticle-based drug delivery systems for cancer treatment. *Biomed. Technol.* 5, 109-122. https://doi.org/10.1016/j.bmt.2023.09.001

7. Feng, S., Dai, Z., et al. 2018. Intake of stigmasterol and β-sitosterol alters lipid metabolism and alleviates NAFLD in mice fed a high-fat western-style diet. *Biochim. Biophys. Acta - Mol. Cell Biol. Lipids.* 1863, 1274–1284. https://doi.org/https://doi.org/10.1016/j.bbalip.2018.08.004

8. Geuli, O., Metoki, N., et al. 2017. Synthesis, Coating and Drug-Release of Hydroxyapatite Nanoparticles Loaded with Antibiotics. *Mater. Chem. B*. 5, 7819–7830. https://doi.org/10.1039/C7TB02105D

9. Gopi, D., Indira, J., et al. 2012. Synthesis of hydroxyapatite nanoparticles by a novel ultrasonic assisted with mixed hollow sphere template method. *Spectrochim. Acta Part A Mol. Biomol. Spectrosc*. 93, 131–134. https://doi.org/10.1016/j.saa.2012.02.033

10. Gray, V., Cole, E., et al. 2014. Use of Enzymes in the Dissolution Testing of Gelatin Capsules and Gelatin-Coated Tablets-Revisions to Dissolution < 711 > and Disintegration and Dissolution of Dietary Supplements < 2040 >. *Dissolution Technol*. 21, 6–19. https://doi.org/10.14227/DT210414P6

11. Kwon, H. J., Shin, K., et al. 2018. Large-scale synthesis and medical applications of uniform-sized metal oxide nanoparticles. *Adv. Mater*., 30(42), 1-24. *Adv. Mater*. https://doi.org/10.1002/adma.201704290

12. Li, Y., Cupo, M., et al. 2017. Enhanced reactive oxygen species through direct copper sulfide nanoparticle-doxorubicin complexation. *Nanotechnology*, 28(50) 1-29. https://doi.org/10.1088/1361-6528/aa967b

13. Maheen, S., Younis, H., et al. 2022. Enhanced Antifungal and Wound Healing Efficacy of Statistically Optimized, Physicochemically Evaluated Econazole-Triamcinolone Loaded Silica Nanoparticles. *Front. Chem*. 10, 1 - 16. https://doi.org/10.3389/fchem.2022.836678

14. Moreno, E.C., Gregory, T.M., et al. 1968. Preparation and Solubility of Hydroxyapatite. *J. Res. Natl. Bur. Stand. Sect. A, Phys. Chem.* 72A, 773–782. https://doi.org/10.6028/jres.072A.052

15. Mulenos, M.R., Lujan, H., et al. 2020. Silver Nanoparticles Agglomerate Intracellularly Depending on the Stabilizing Agent: Implications for Nanomedicine Efficacy. *Nanomaterials*. 10, 1-15. https://doi.org/10.3390/nano10101953

16. Muscas, G., Singh, G., et al. 2015. Tuning the Size and Shape of Oxide Nanoparticles by Controlling Oxygen Content in the Reaction Environment: Morphological Analysis by Aspect Maps. *Chem. Mater.* 27, 1982–1990. https://doi.org/10.1021/cm5038815

17. Pan, C., Liu, Y., et al. 2018. Theranostic pH-sensitive nanoparticles for highly efficient targeted delivery of doxorubicin for breast tumor treatment. *Int. J. Nanomedicine.* 13, 1119-1137. https://doi.org/10.2147/IJN.S147464

18. Šoltys, M., Kovačík, P., et al. 2019. Effect of solvent selection on drug loading and amorphisation in mesoporous silica particles. *Int. J. Pharm.* 555, 19–27. https://doi.org/10.1016/j.ijpharm.2018.10.075

19. Swain, S.K., Dorozhkin, S. V, et al. 2012. Synthesis and dispersion of hydroxyapatite nanopowders. *Mater. Sci. Eng. C.* 32, 1237–1240. https://doi.org/10.1016/j.msec.2012.03.014

20. Venkatesan, J., Lowe, B., et al. 2015. Isolation and characterization of nano-hydroxyapatite from salmon fish bone. *Materials*. 8(8), 5426-5439. https://doi.org/10.3390/ma8085253

21. Yang, Y. H., Liu, C. H., et al. 2013. Hollow mesoporous hydroxyapatite nanoparticles (hmHANPs) with enhanced drug loading and pH-responsive release properties for intracellular drug delivery. *J. Mater. Chem. B.* 1(19), 2447-2450. https://doi.org/10.1039/C3TB20365D

22. Yu, J., Chu, X., et al. 2014. Preparation and characterization of antimicrobial nano-hydroxyapatite composites. *Mater. Sci. Eng. C*. 37, 54-59. https://doi.org/10.1016/j.msec.2013.12.038

23. Zhang, X.F., Liu, Z.G., et al. 2016. Silver nanoparticles: Synthesis, characterization, properties, applications, and therapeutic approaches. *Int. J. Mol. Sci.* 17, 1–34. https://doi.org/10.3390/ijms17091534